

Insight into association reactions on metal surfaces: Density-functional theory studies of hydrogenation reactions on Rh(111)

Zhi-Pan Liu and P. Hu^{a)}

School of Chemistry, The Queen's University of Belfast, Belfast, BT9 5AG United Kingdom

Ming-Hsien Lee

Department of Physics, Tamkang University, Tamsui, 25137, Taiwan

(Received 21 April 2003; accepted 25 June 2003)

Hydrogenation reaction, as one of the simplest association reactions on surfaces, is of great importance both scientifically and technologically. They are essential steps in many industrial processes in heterogeneous catalysis, such as ammonia synthesis ($N_2 + 3H_2 \rightarrow 2NH_3$). Many issues in hydrogenation reactions remain largely elusive. In this work, the NH_x ($x = 0, 1, 2$) hydrogenation reactions ($N + H \rightarrow NH$, $NH + H \rightarrow NH_2$ and $NH_2 + H \rightarrow NH_3$) on Rh(111) are used as a model system to study the hydrogenation reactions on metal surfaces in general using density-functional theory. In addition, C and O hydrogenation ($C + H \rightarrow CH$ and $O + H \rightarrow OH$) and several oxygenation reactions, i.e., $C + O$, $N + O$, $O + O$ reactions, are also calculated in order to provide a further understanding of the barrier of association reactions. The reaction pathways and the barriers of all these reactions are determined and reported. For the C, N, NH, and O hydrogenation reactions, it is found that there is a linear relationship between the barrier and the valency of R ($R = C, N, NH, \text{ and } O$). Detailed analyses are carried out to rationalize the barriers of the reactions, which shows that: (i) The interaction energy between two reactants in the transition state plays an important role in determining the trend in the barriers; (ii) there are two major components in the interaction energy: The bonding competition and the direct Pauli repulsion; and (iii) the Pauli repulsion effect is responsible for the linear valency-barrier trend in the C, N, NH, and O hydrogenation reactions. For the $NH_2 + H$ reaction, which is different from other hydrogenation reactions studied, the energy cost of the NH_2 activation from the IS to the TS is the main part of the barrier. The potential energy surface of the NH_2 on metal surfaces is thus crucial to the barrier of $NH_2 + H$ reaction. Three important factors that can affect the barrier of association reactions are generalized: (i) The bonding competition effect; (ii) the local charge densities of the reactants along the reaction direction; and (iii) the potential energy surface of the reactants on the surface. The lowest energy pathway for a surface association reaction should correspond to the one with the best compromise of these three factors. © 2003 American Institute of Physics. [DOI: 10.1063/1.1602054]

I. INTRODUCTION

Association and dissociation reactions on solid surfaces constitute the two fundamental types of chemical reactions in heterogeneous catalysis. In the last several decades, great efforts have been made in order to understand dissociation reactions.¹⁻⁹ In particular, systematic studies on H_2 dissociation on metal surfaces have been carried out theoretically and a significant insight into the reaction has been obtained.^{3,4} Now theoretical studies have moved on to large, heavy molecules, such as CH_4 , CO, N_2 , and NO and the reaction site has been extended from close-packed surfaces to surface defects, such as monatomic steps and kinks.⁵⁻⁸ To date some general features of dissociation reactions have been obtained.⁴⁻⁶ However, due to the more complex nature involved in the adsorbed reactants on surfaces, the understanding of the association reactions is still limited.^{4,9} Obviously, a systematic study on association reactions is needed and also timely.

Hydrogenation is a fundamental association reaction in heterogeneous catalysis. In many industrial processes, such as ammonia synthesis ($N_2 + 3H_2 \rightarrow 2NH_3$)¹⁰⁻¹³ and Fischer-Tropsch ($CO + H_2 \rightarrow \text{Hydrocarbons} + H_2O$),¹³⁻¹⁶ hydrogenation reactions are the essential steps to produce the final products, and in others, such as NO reduction by H_2 ($2NO + H_2 \rightarrow N_2 + H_2O$), they are used to remove unwanted species on catalysts to prevent the catalysts being poisoned. Hydrogenation reactions in heterogeneous catalysis contain normally several continual steps. Taking ammonia synthesis as an example, it is generally accepted that ammonia synthesis consists of the following elementary steps:¹⁰⁻¹³ (i) The dissociations of N_2 and H_2 ; and (ii) the stepwise hydrogenation reactions, namely, $N + H \rightarrow NH$, $NH + H \rightarrow NH_2$ and $NH_2 + H \rightarrow NH_3$. In spite of the great industrial importance, stepwise hydrogenation reactions were less studied, and many issues remain largely elusive. In this work, we studied NH_x hydrogenations and other reactions on Rh(111) and the results were compared with our previous NH_x hydrogenations on Ru(0001).¹⁷ By detailed analyses, insight into the barrier of association reactions on metals was obtained.

^{a)} Author to whom correspondence should be addressed. Electronic mail: p.hu@qub.ac.uk

Because of their relevance to ammonia synthesis and relative simplicity, NH_x hydrogenation reaction is a good model system for the study of hydrogenation reactions in general. Recently, we have calculated NH_x hydrogenation reactions on Ru(0001) using density-functional theory (DFT),¹⁷ aiming to obtain a comprehensive picture for ammonia synthesis on Ru, a promising alternative to the traditional Fe catalysts.^{10–13,17} We found that the highest barrier for these reactions is in the $\text{NH} + \text{H} \rightarrow \text{NH}_2$ step, which is up to 1.28 eV. Even taking into account the effect of surface defects, such as steps, the hydrogenation reaction barrier is still around 0.8 eV. Our results showed that hydrogenation barriers are higher than the reported barrier for N_2 dissociation on Ru, the believed rate-determining step in ammonia synthesis.¹⁸ The barrier for N_2 dissociation on Ru(0001) was determined to be 1.36 eV by DFT.¹⁹ Later, combined STM with DFT calculations Dahl *et al.* found that the barrier of N_2 dissociation on Ru monatomic steps was as low as 0.4 eV.⁵ It was estimated that N_2 dissociation on steps is at least 9 orders of magnitude faster than that on terrace sites.⁵

The high barrier of hydrogenation reactions has motivated the current work and promoted some questions. Firstly, is it in general that the hydrogenation reactions, e.g., $\text{NH} + \text{H}$ reaction, have high barriers on late transition metals? Or is it only true on Ru? Since it is known that only Fe and Ru are good catalysts for ammonia synthesis, the study of other less active metals may provide useful information on ammonia synthesis. Secondly, if the hydrogenation barriers are generally high, what then is the physical origin? Considering that hydrogenation reactions may be the simplest association reactions on metal surfaces, a deeper understanding on hydrogenation reactions is of fundamental significance. In this work, we selected Rh(111) surface to study the NH_x hydrogenations. Rh is on the right-hand side of Ru in the periodic table and is known to be a poorer catalyst for ammonia synthesis than Ru. It should be mentioned that Rh is widely used as a NO reduction catalyst.^{20–22} The NH_x hydrogenation reactions studied here are also of importance to the chemistry of NO reduction.

This paper is organized as follows: Calculation methods are described in Sec. II. In Sec. III, calculation results of all hydrogenation reactions are presented. We also performed the C and O hydrogenation reactions and the results are compared with the N, NH hydrogenation reactions. In Sec. IV, the result of detailed analyses to understand the high barrier of the hydrogenation reactions is reported. Implications to the barrier of association reactions in general are also discussed. Conclusions are summarized at the end of this paper.

II. CALCULATION METHODS

A generalized gradient approximation²³ was utilized in all the calculations. Electronic wave functions were expanded in a plane wave basis set and the ionic cores were described by ultrasoft pseudopotentials.²³ The program used is CASTEP.²⁴ The surface is modeled by three layers of Rh(111), while all the layers were fixed in optimized bulk positions. The effect of surface relaxation was checked and it was found to be rather small to the barriers⁷ (less than 0.1 eV, see Ref. 25). The vacuum region between slabs is 10 Å and

TABLE I. The most stable adsorption site and the corresponding adsorption energy for N, NH, NH_2 , NH_3 , and H species on Rh(111). The bond length between the species with the surface atom is also listed. The experimental value on the NH_3 adsorption on Rh(111) (Ref. 37), where the comparison is possible, is well consistent with the current calculation result.

	Adsorption site	Bond length (Å)	E_{ad} (eV)
N	hcp	1.930 (N–Rh)	4.90
NH	hcp	1.990 (N–Rh)	4.39
NH_2	bridge	2.092 (N–Rh)	2.73
NH_3	top	2.129 (N–Rh)	0.87 ^a
H	fcc	1.842 (H–Rh)	2.94

^aExpt. 0.90 ± 0.03 eV (Ref. 37).

a cut-off energy 340 eV was used. For all the hydrogenation reactions $3 \times 2 \times 1$ **k** point sampling for $p(2 \times 3)$ unit cell within the surface Brillouin zone was used, which is large enough to avoid lateral interaction between the adsorbates in adjacent unit cells. Some calculations in Sec. IV for the purpose of analysis was performed in $p(2 \times 2)$ unit cell with $3 \times 3 \times 1$ **k** point sampling. Convergence check has been performed by increasing **k** point sampling up to $4 \times 4 \times 1$ for the $p(2 \times 2)$ unit cell and $3 \times 3 \times 1$ for the $p(2 \times 3)$ unit cell. Previous work^{7,26–32} showed that this calculation setup affords enough accuracy.

Transition states (TSS) were searched by constraining the distance of two reactants (e.g., H– NH_x distance) with the so-called constrained minimization technique.^{26,33} The TS is identified when (i) the force on the atoms vanish and (ii) the energy is a maximum along the reaction coordinate, but a minimum with respect to all remaining degrees of freedom. All the reaction barriers are referenced to the most stable initial states (ISs), which correspond to the low coverage reaction condition [1/6 monolayer (ML) NH_x and 1/6 ML H].

III. RESULTS

A. NH_x and H adsorption on Rh(111)

We firstly investigated the adsorption properties of H atom and NH_x ($x=0,1,2,3$) species on Rh(111) at a 1/4 ML coverage. Table I lists the calculated chemisorption energies (E_{ad}) and the important structural parameters corresponding to the most stable configuration of the adsorbates on Rh(111). It shows that on Rh(111) N, NH, and H prefer the threefold hollow site: N and NH are more stable at the hcp hollow site, and H slightly favors the fcc hollow site. NH_2 and NH_3 prefer less coordinated sites on the surface: NH_2 adsorbs preferentially on the twofold bridge site, and NH_3 is more stable on the top site. Table I also shows clearly that as N is hydrogenated (i.e., x increases), the NH_x adsorption energy decreases gradually. In consistent with the chemisorption energy, the Rh– NH_x bond becomes longer as x increases. Comparing to E_{ad} of NH_x adsorption on Ru(0001),¹⁷ we found that the NH_x adsorption energies on Rh(111) are generally smaller. In particular, E_{ad} of N atom on Rh(111) is about 0.8 eV smaller than that on Ru(0001). This is consistent with the general consensus that as the metal d occupancy increases (the d orbitals of Rh is more occupied than that of Ru), the covalent bonding ability of the metal surface de-

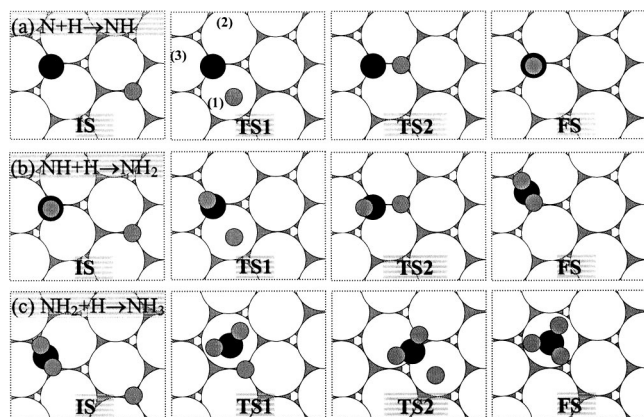


FIG. 1. Illustration of the IS, TSs, and FS of the $N+H$, $NH+H$, and NH_2+H reactions on Rh(111). For each reaction, the most stable IS, the two TS and the most stable FS are shown. TS1 is more stable than TS2.

creases. The most stable configuration of the species on the surface will be taken as the IS for the hydrogenation reactions, which are studied in the following subsection.

B. $NH_x+H \rightarrow NH_{x+1}$ reactions

To map out the most likely reaction pathway for each hydrogenation reaction, we searched all the possible TSs for each hydrogenation reaction. We found that there are two TSs for each hydrogenation reaction. In Fig. 1 we illustrate the IS, TSs, and final state (FS) for $N+H$ [Fig. 1(a)], $NH+H$ [Fig. 1(b)] and NH_2+H [Fig. 1(c)] reactions. For each reaction, two TSs are shown: We label the most stable TS as TS1 and the less stable one as TS2. Our results are presented in the following.

1. $N+H \rightarrow NH$ and $NH+H \rightarrow NH_2$

We will discuss $N+H \rightarrow NH$ and $NH+H \rightarrow NH_2$ together because the TSs of these two reactions are similar, as shown in Figs. 1(a) and 1(b). At the TSs N or NH stays near the hcp hollow site, which is also the most stable IS for N or NH. The TS1 differs from the TS2 by the H position: The H atom is on the off-top site at the TS1, while it is at a nearby fcc hollow site at the TS2. Thus, as shown in Fig. 1, at the TS1 N (or NH) and H share bonding with one surface Rh atom, and at the TS2 two Rh atoms are shared. It has been shown that such a bonding sharing between adsorbates will induce a repulsion between two adsorbates, the so-called bonding competition effect.^{34–36} This effect was found to play an important role in determining the height of reaction barriers.^{7,26} We will also discuss this effect in Sec. IV.

The barriers (E_a) for $N+H$ and $NH+H$ reactions were determined and listed in Table II. The important structural parameters of the TS1 are listed in Table III. E_a^{TS1} is the barrier corresponding to TS1 and E_a^{TS2} corresponding to TS2. As shown in Table II, E_a^{TS1} is 0.99 eV in $N+H$ reaction, and 1.25 eV in $NH+H$ reaction. It is noticed that these values on Rh(111) are very similar to the barriers on Ru(0001) [$N+H$ reaction: $E_a = 1.13$ eV and $NH+H$ reaction: $E_a = 1.28$ eV on Ru(0001)¹⁷]. The common feature is that on both Ru and Rh surfaces, $NH+H$ reaction is more difficult than $N+H$ reaction. Table II also shows that the energy difference between

TABLE II. Reaction barriers for the N, NH, NH_2 , C, and O hydrogenation reactions. Because there are two TSs, named TS1 and TS2 (Fig. 1) for each reaction, two corresponding barriers (E_a^{TS1} and E_a^{TS2}) are calculated with respect to the most stable IS. The unit of the barrier is eV.

	E_a^{TS1}	E_a^{TS2}
$N+H \rightarrow NH$	0.99	1.22
$NH+H \rightarrow NH_2$	1.25	1.29
$NH_2+H \rightarrow NH_3$	1.24	1.32
$C+H \rightarrow CH$	0.72	0.98
$O+H \rightarrow OH$	1.36	1.36

E_a^{TS1} and E_a^{TS2} is 0.23 eV in $N+H$ reaction, and the difference is only 0.04 eV in $NH+H$ reaction. It implies that for the $N+H$ reaction the reaction pathway involved with TS1 is favored, while for the $NH+H$ reaction both TS1 and TS2 may be accessible during the reaction.

2. $NH_2+H \rightarrow NH_3$

The NH_2+H is different from the reactions of $N+H$ and $NH+H$ regarding the TS structure. This is clearly shown in Fig. 1. At the TS1 of NH_2+H reaction, NH_2 is on a off-top site, and the H atom is near the fcc site. At the TS2, which is less stable, NH_2 stays near the bridge site and the H atom is at the nearby top site. The determined E_a corresponding to these two TSs are similar: E_a^{TS1} is 1.24 eV and E_a^{TS2} is 1.32 eV. Similar to the results on Ru(0001), the NH_2+H reaction on Rh(111) also has a high barrier, which is almost identical to that of $NH+H$ reaction.

The total energy profile for all the NH_x hydrogenation reactions on Rh(111) is summarized in Fig. 2, in which the energy profile of NH_x hydrogenation on Ru(0001)¹⁷ is also included for comparison. It shows that the energetics of NH_x hydrogenation on Rh(111) and Ru(0001) surfaces appear to be very similar. For example, on both surfaces NH is the most stable intermediate species and the $NH+H$ reaction is the most difficult step. However, it is interesting to notice that on Ru(0001) NH_2 is particularly unstable, due to a small decomposition barrier, about 0.6 eV for $NH_2 \rightarrow NH+H$ reaction. On Rh(111), NH_2 is quite stabilized: The hydrogenation of NH to NH_2 has a barrier 1.25 eV, and the decomposition of NH_2 to NH is still hindered by 1.00 eV.

TABLE III. Important geometrical parameters for the most stable TS of C+H, N+H, NH+H and O+H reactions (R is C, N, NH or O). At the TSs the C, N, NH, and O are all at the hollow sites on Rh(111) and the H is near the top site. The Rh⁽¹⁾, Rh⁽²⁾, and Rh⁽³⁾ represent the Rh atoms involved in bonding with the TS complex, shown in Fig. 1(a)—TS1. The unit of the distances is Å.

	C+H→CH	N+H→NH	NH+H→NH ₂	O+H→OH
R–Rh ⁽¹⁾	1.962	2.017	2.080	2.088
R–Rh ⁽²⁾	1.903	1.945	2.026	2.074
R–Rh ⁽³⁾	1.903	1.945	2.026	2.075
H–Rh ⁽¹⁾	1.618	1.629	1.642	1.646
H–R	1.636	1.516	1.445	1.435

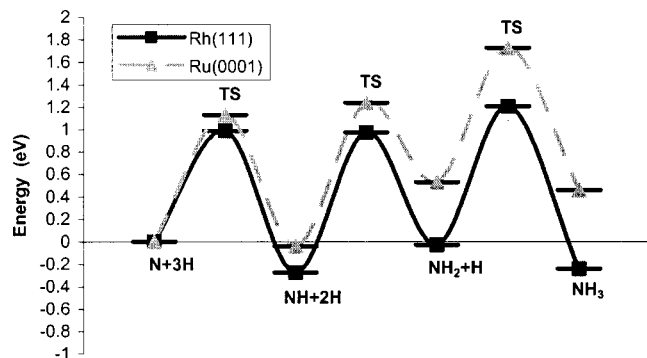


FIG. 2. The overall energy diagram for the NH_x ($x=0,1,2$) hydrogenation on Rh(111). For comparison, the previous results on Ru(0001) (Ref. 17) are also shown. For each metal surface, the state of the separated N and H atom adsorption on the surface is set as the energy zero.

C. $\text{C}+\text{H}\rightarrow\text{CH}$ and $\text{O}+\text{H}\rightarrow\text{OH}$ reactions

To obtain a better understanding of the hydrogenation reactions regarding, in particular, the reason for the high barrier of the $\text{NH}+\text{H}$ reaction, we also investigated $\text{C}+\text{H}\rightarrow\text{CH}$ and $\text{O}+\text{H}\rightarrow\text{OH}$ reaction on Rh(111). Similarly, we have located the ISs and TSs for $\text{C}+\text{H}$ and $\text{O}+\text{H}$ reactions on Rh(111). We found that $\text{C}+\text{H}$ and $\text{O}+\text{H}$ reactions are very similar to the $\text{N}+\text{H}$ and $\text{NH}+\text{H}$ reactions. There are also two TSs in each reaction of $\text{C}+\text{H}$ and $\text{O}+\text{H}$, which are almost the same as those depicted in Fig. 1(a) for the $\text{N}+\text{H}$ reaction. E_a^{TS1} and E_a^{TS2} of the $\text{C}+\text{H}$ and $\text{O}+\text{H}$ reactions were calculated, and the results are listed Table II. The important structural parameters of the TS1 are listed in Table III.

By comparison of the C and O hydrogenation reactions with those of N and NH, we have obtained some useful clues for the high barrier of the $\text{NH}+\text{H}$ reaction. As shown in Table II, the $\text{C}+\text{H}$ reaction on Rh(111) is the easiest reaction with a low barrier of 0.72 eV, while the $\text{O}+\text{H}$ reaction is the most difficult one with a barrier almost twice larger than that of $\text{C}+\text{H}$ reaction. The barriers of $\text{N}+\text{H}$ and $\text{NH}+\text{H}$ reactions lie in between the $\text{C}+\text{H}$ and $\text{O}+\text{H}$ reactions. Moreover, we have identified a good linear relationship between the barrier of C, N, and O hydrogenation reactions and the valency of C, N, and O, as plotted in the dotted line of Fig. 3 ($E_{\text{int}}^{\text{TS}}$ is defined in Sec. IV, see discussion below). It shows that as the valency of R ($\text{R}=\text{C}, \text{N}, \text{and O}$) decreases, the barrier increases linearly. Conventionally, the NH valency is often considered to be 2, the same as that of O atom. From the barrier of the $\text{NH}+\text{H}$ reaction, using Fig. 3 we deduced the valency of NH to be about 2.2, which is, as expected, close to 2.

IV. DISCUSSIONS

A. Origin of the valency-barrier trend in C, N, NH, and O hydrogenation reactions

As reported above, the hydrogenation reactions of C, N, NH, and O possess similar TS structures and the barrier is a linear function of the valency of these species. It is obvious that the valency-barrier trend is the key to understand the

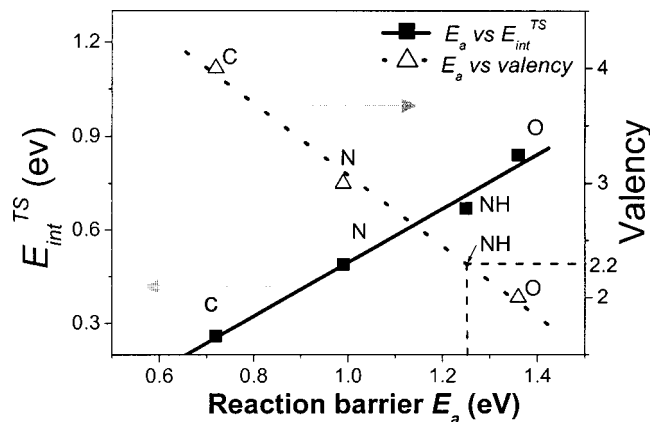


FIG. 3. The plot of the E_a -valency relationship (dotted line) and the E_a - $E_{\text{int}}^{\text{TS}}$ (solid line) relationship for the C, N, NH, and O hydrogenation reactions on Rh(111). The term of $E_{\text{int}}^{\text{TS}}$ is defined in Sec. IV, Eq. (1) (see discussion below). The arrows point out the corresponding y axis of the lines.

high barrier of the $\text{NH}+\text{H}$ reaction. Below, we will focus on the origin of the valency-barrier trend. The NH_2+H reaction will be discussed in the next subsection.

As a starting point, we have analyzed the electronic structure of the C, N, NH, and O adsorption on Rh(111) using the local density of states (LDOS) plot,³⁸ as shown in Fig. 4. The LDOS of R ($\text{R}=\text{C}, \text{N}, \text{NH}, \text{and O}$) on Rh(111) was calculated by cutting a small volume with a 0.3 Å radius around the R center (for NH, it is the N atom). Figure 4 shows that the main difference between different LDOSs lies at the energy region from -7 to -5 eV. This region contains mainly the p orbitals of R mixing with the metal d band, namely the p - d bonding region. In the O LDOS only one peak with a high intensity in the low energy area is seen at the p - d bonding region. On going from O to C, the p - d bonding peak shifts gradually up in energy and the intensity of the peaks becomes smaller. It indicates that the p orbitals of the lower valency adsorbate are more localized around the adsorbate center in these species. It should be mentioned that the NH LDOS is largely overlapped with that of O, and thus it is not shown in Fig. 4. Based on the LDOS plots, we may qualitatively understand the valency-barrier trend of Fig. 3 as follows. Required by Pauli principle,⁴⁰ the occupied $1s$ state

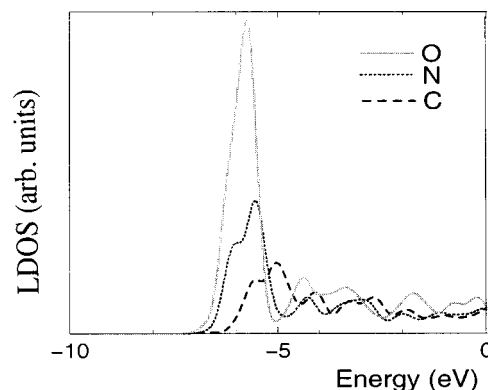


FIG. 4. Local density of states (LDOS) of the C, N, O adsorption on Rh(111). Each LDOS is calculated by cutting a small volume with a 0.3 Å radius around the atom center.

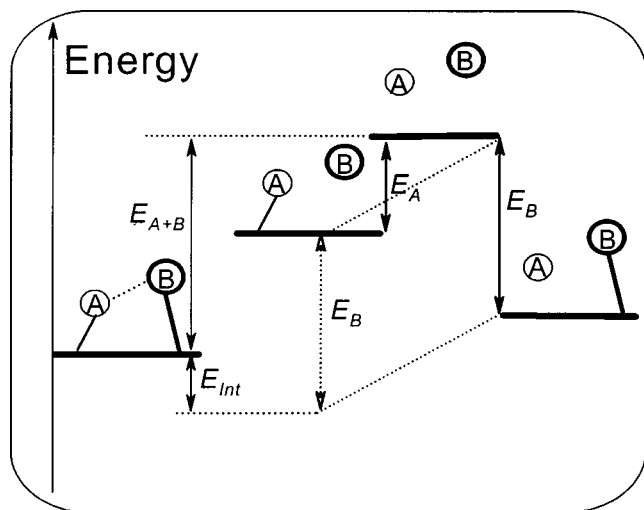


FIG. 5. Illustration of the energy decomposition of a $A+B$ coadsorption system on metal surfaces. The figure is used to help the explanation of each term in Eq. (1).

of H atom must be firstly orthogonal to the occupied p - d bonding states of R when the adsorbed H atom comes to react with R. As shown in the LDOS, the p - d bonding states of the lower valency adsorbate have higher electron densities localized around the adsorbate, which will induce a larger Pauli repulsion between the coming H $1s$ states and the p - d bonding states of the adsorbate. Therefore, the Pauli repulsion for the low valency adsorbate reacting with H is larger, and consequently the hydrogenation barrier is higher.

To obtain a further understanding, we have used the barrier decomposition scheme to analyze the reaction barrier quantitatively. The barrier decomposition scheme was introduced in our previous work⁷ and has been found to be very useful to provide insight into the chemical reactions on surfaces. As shown in Fig. 5, for any coadsorption system of reactants A and B , such as a TS, the total chemisorption energy, E_{A+B}^{TS} , can be written:

$$E_{A+B}^{TS} = E_A^{TS} + E_B^{TS} - E_{int}^{TS}, \quad (1)$$

where E_A^{TS} (E_B^{TS}) is the chemisorption energy of A (B) at the TS without B (A), E_{int}^{TS} is the energy term required to make up the overall E_{A+B}^{TS} , which is a quantitative measure of the interaction between A and B in the coadsorption system. Similarly, for the IS we write:

$$E_{A+B}^{IS} = E_A^{IS} + E_B^{IS} - E_{int}^{IS}. \quad (2)$$

Then the reaction barrier E_a is

$$E_a = E_{A+B}^{IS} - E_{A+B}^{TS} = \Delta E_A + \Delta E_B + \Delta E_{int}, \quad (3)$$

where $\Delta E_A = E_A^{IS} - E_A^{TS}$; $\Delta E_B = E_B^{IS} - E_B^{TS}$; $\Delta E_{int} = E_{int}^{TS} - E_{int}^{IS}$. ΔE_A (ΔE_B) is the energy cost for reactant A (B) moving from its position in the IS to the TS without B (A). The interaction energy difference is represented by ΔE_{int} . Generally, it is reasonable to omit E_{int}^{IS} if the coverage is low (reactants A and B are well separated). Thus ΔE_{int} is mainly determined by E_{int}^{TS} ($\Delta E_{int} \approx E_{int}^{TS}$).

Using Eq. (3), we decomposed the reaction barriers of C, N, NH, and O hydrogenation into three components and the results are listed in Table IV. It shows that the E_{int}^{TS} plays an important role in determining E_a of hydrogenation reactions. Two main features can be seen clearly: (i) In the TS1, the change in the first two terms, ΔE_R and ΔE_H , is very small from one reaction to another. ΔE_R is very small, which is due to the fact that R is at the same hollow site in the TS as that in the IS. ΔE_H comes mainly from the chemisorption energy difference of the H atom from the initial fcc hollow site to the top site (0.44 eV). Importantly, the third term, ΔE_{int} (i.e., $\sim E_{int}^{TS}$), is increased proportionally with the decrease of the R valency. This indicates clearly that it is the E_{int}^{TS} that determines the trend of the hydrogenation barriers. (ii) Comparing the barrier decomposition results in the TS1 and the TS2, we can see that E_{int}^{TS} in the TS2 is always larger than that in the TS1. This is the reason for E_a^{TS1} being smaller than E_a^{TS2} .

Because E_a of the hydrogenation reactions is largely determined by E_{int}^{TS} , it is worth discussing further the physical meaning of E_{int}^{TS} . As it is shown, E_{int}^{TS} is normally a positive term in surface reactions, which indicates the repulsive nature of the interaction between two reactants. There are two major repulsive interactions between reactants on surfaces.^{7,26,34-36} The first one is the indirect bonding competition effect, which was introduced by Feibelman.³⁹ This effect is caused by the two reactants sharing bonding with the same surface atoms: When one adsorbate bonds with a metal atom, the metal atom becomes inert for further bonding with the second species. The second component is the direct Pauli repulsion between two reactants.⁴⁰ The Pauli repulsion effect is of short range and is dominant when two adsorbates are very close, e.g., within 2.5 Å. It should be mentioned that E_{int}^{TS} may contain other components, but they are believed to be rather small.³⁵

Since both the bonding competition effect and the direct Pauli repulsion effect contribute to E_{int}^{TS} , an interesting question arises: Which effect is responsible for the linear valency-barrier relationship? We have used the following method to

TABLE IV. The barrier decomposition of the C+H, N+H, NH+H, and O+H reactions. Each term is defined in Eq. (3) and discussed in the text.

	TS1				TS2			
	ΔE_R	ΔE_H	E_{int}^{TS}	E_a^{TS1}	ΔE_R	ΔE_H	E_{int}^{TS}	E_a^{TS2}
C+H→CH	0.02	0.44	0.26	0.72	0.04	0.14	0.79	0.98
N+H→NH	0.05	0.45	0.49	0.99	0.09	0.16	0.96	1.22
NH+H→NH ₂	0.11	0.46	0.67	1.25	0.14	0.15	1.00	1.29
O+H→OH	0.08	0.43	0.84	1.36	0.21	0.01	1.14	1.36

estimate the magnitude of the bonding competition effect of a R+H coadsorption system without the interference of the direct Pauli repulsion effect: (i) Both R and H were optimized at a hcp hollow site in a separate $p(2\times 2)$ unit cell and their chemisorption energies were calculated, namely E_R and E_H ; and (ii) the total chemisorption energy, E_{R+H} of R+H coadsorption were calculated, in which R is at a hcp hollow site and H at a neighboring hcp site in $p(2\times 2)$ unit cell (they will share two surface atoms in such a unit cell) and both were fixed at the structure (i). Then we define

$$E_{\text{int}} = E_R + E_H - E_{R+H}, \quad (4)$$

as the interaction energy. Because of the large separation of R and H in this case, i.e., the distance between R and H being around 2.7 Å, then E_{int} measures mainly the bonding competition effect. The E_{int} for C, N, and O are found to be very close: for C, 0.21 eV; for N, 0.22 eV; for O, 0.18 eV. This indicates that the bonding competition effect between R and H is not so sensitive to the R valency. Thus, this implies that the direct Pauli repulsion effect may be responsible for the valency-barrier trend. The small magnitude of the bonding competition effect between R and H is interesting, considering that the bonding competition effect is large for other multivalency pairs on metals as reported in our previous paper. For example, we showed that E_{int} for a C–O pair on Rh(111) is 0.45 eV, and it is even higher to be 0.63 eV on Pd(111).⁷ In fact, considering that the valency of H atom is only one, and the H atom does not covalently bond with the surface so strongly compared to other multivalency adsorbates, we suggest that the bonding competition of other adsorbates with the H atom may always be small.

Indeed, our further calculations show that the direct Pauli repulsion effect is strongly affected by the reactant valency. We performed a similar calculation using the same method as described in the last paragraph except that the H now is put at its optimized top site, rather than the neighboring hcp site. In such structure the distance between R and H is around 1.6 Å, which is within the range of the direct Pauli repulsion. The calculated E_{int} for R–H pairs using Eq. (4) are as follows: C–H, 0.28 eV; N–H, 0.54 eV; O–H, 0.78 eV. These values agree very well with the $E_{\text{int}}^{\text{TS}}$ of TS1 in Table IV. Moreover, there is also a linear relationship between E_{int} and the R valency. This indicates that the direct Pauli repulsion effect is responsible for the valency-barrier trend. These quantitative analyses are consistent with our qualitative understanding described above using LDOS: The higher the local charge densities of adsorbates, the larger the Pauli repulsion between the adsorbates and hence the higher the barrier. The valency-barrier trend is basically a result of the Pauli repulsion effect. The high barrier of the NH+H reaction is the consequence of the low valency of NH.

It should be mentioned that the barrier decomposition results in Table IV also show $E_{\text{int}}^{\text{TS}}$ in the TS2 being larger than that in the TS1. This may be due to the fact that in the TS2 two surface atoms are shared by the reactants, while in the TS1 only one surface atom is shared. Consequently, TS2 is less stable than the TS1.

The valency-barrier trend may not be limited in the hydrogenation reactions. To check the validity of the valency

effect for other association reactions, we have performed three oxygenation reactions: $\text{C}+\text{O}\rightarrow\text{CO}$, $\text{N}+\text{O}\rightarrow\text{NO}$, and $\text{O}+\text{O}\rightarrow\text{O}_2$ on Rh(111). The reaction barriers have been determined to be 1.59, 2.17, and 2.51 eV for C+O, N+O, and O+O reactions, respectively. It is clear that the valency-barrier trend is still present in the series of oxygenation reactions: The lower the valency of reactants, the higher the oxygenation barrier. These results show again that the direct Pauli repulsion effect between reactants plays an important role in determining the barrier of surface association reactions.

B. Origin of the barrier in NH_2+H reaction

According to the valency-barrier trend, it is expected that the barrier of NH_2+H reaction should be higher than that of $\text{NH}+\text{H}$ reaction. However, on Rh(111) the barrier of NH_2+H reaction is 0.01 eV lower than that of the $\text{NH}+\text{H}$ reaction, and on Ru(0001) it is also 0.03 eV lower. Naturally, one may ask why NH_2+H reaction is special.

To answer this question, we compared the NH_2+H reaction with the other hydrogenation reactions. Two interesting features were observed: (i) At the IS, NH_2 adsorbs at the twofold bridge site, while C, N, NH, and O adsorb on threefold hollow sites; (ii) at the TS1, NH_2 moves to a top site to react with H [Fig. 1(c)], while C, N, NH, and O all stay at the hollow sites to react with H. These two features indicate that the NH_2+H reaction possesses its own characteristics, being different from the other hydrogenation reactions discussed in the last section. We decomposed the barrier of NH_2+H reaction using Eq. (3). Indeed, the barrier decomposition analysis reveals the following distinct features of NH_2+H reaction: Firstly, the energy cost for NH_2 to be activated from the IS to the TS, ΔE_{NH_2} , was found to be 0.72 eV, significantly higher than ΔE_R (R=C, N, NH, and O) of the R+H reactions. ΔE_R is small because C, N, NH, and O are all on the hollow sites in both ISs and TSs in the reactions. In contrast, in the NH_2+H reaction NH_2 is activated from the bridge site (IS) to the off-top site (TS), which costs a significant amount of energy because of the corrugated potential energy surface of NH_2 on Rh(111). ΔE_{NH_2} is, in fact, the major component of the barrier of the NH_2+H reaction. Secondly, $E_{\text{int}}^{\text{TS}}$ was calculated to be 0.42 eV, being smaller than that for the $\text{NH}+\text{H}$ reaction (0.67 eV) even though the valency of NH_2 is supposed to be lower than that of NH. This is because at the TS NH_2 is less coordinated on the surface compared to the C, N, NH, and O. The low coordination of NH_2 on the surface changes the electronic distribution of NH_2 and thus varies effectively the valency of NH_2 . As a result, the incurred Pauli repulsion between NH_2 and H is reduced. Michaelides and Hu have studied the bonding variation of O atom adsorption on Pt(111) as the O goes from a hollow site to a bridge site and to a top site: it was shown that during the site-shifting the local charge densities on the O are gradually reduced.³⁸ This is expected to be quite general for other electronegative adsorbates on metal surfaces. As we discussed above, the small charge densities on the adsorbate will incur small Pauli repulsion in the reaction and thus leads to a small barrier.

A unique feature of $\text{NH}_2 + \text{H}$ reaction is that its barrier is strongly related to the potential energy surface of NH_2 and not significantly affected by the Pauli repulsion between reactants. For the $4d$ metals, such as Ru and Rh, we have found that the potential energy surface of NH_2 is very corrugated and hence the hydrogenation barriers are consequently high, which is not the case on Pt. Because the $5d$ orbitals of Pt are much more extended, the potential energy surface of many adsorbates on Pt is normally quite flat. Indeed, the barrier of $\text{NH}_2 + \text{H}$ barrier on Pt(111) is only 0.7 eV, as reported by previous DFT calculations,³⁸ being much smaller than those on Ru(0001) and Rh(111). It should be mentioned that the barriers for the $\text{NH} + \text{H}$ reaction are quite similar on Pt(111), Ru(0001), and Rh(111) (the barrier of $\text{NH} + \text{H}$ reaction on Pt(111) was reported to be 1.3 eV³⁸), which can be readily understood by considering that the barrier of $\text{NH} + \text{H}$ reaction is to a large extent determined by the valency of NH and not so sensitive to the metal surfaces. The reaction of $\text{OH} + \text{H} \rightarrow \text{H}_2\text{O}$ on metals is another example, in which the potential energy surface of reactants largely determines the reaction barrier. Similar to the $\text{NH}_2 + \text{H}$ reaction, in the $\text{OH} + \text{H}$ reaction the OH needs to be activated from one site (normally bridge site) at the IS to another site at the TS (normally top site).^{30,38} Again, on Pt(111) the potential energy of OH is very flat and thus the barrier of the $\text{OH} + \text{H}$ reaction on Pt(111) is very small (0.2 eV),³⁰ whereas on Ru(0001), the potential energy surface of OH is corrugated and the barrier of $\text{OH} + \text{H}$ reaction is quite high, being about 1 eV.

C. General implication for the association reactions on metal surfaces

Because hydrogenation reactions are prototypical association reactions on surfaces, our results should have some implications on the barrier of association reactions in general. To a large extent, three important factors can affect the barrier of association reactions.

(i) The bonding competition effect. The bonding competition energy cost is induced whenever two reactants bond with the same surface atoms in the reaction. It was recently found that the bonding competition effect is important in understanding the high catalytic activity of surface defects.^{5,7,36} For instance, $\text{C} + \text{O} \rightarrow \text{CO}$ on Ru was observed to occur at a much lower temperature with the presence of surface steps.⁴¹ From DFT calculations, it was found that on steps two reactants can react without sharing surface atoms, while on flat surfaces they have to share bonding with one surface atom.^{5,7,36} For the hydrogenation reaction studied here, we found that the bonding competition effect is not significant due to the intrinsic small bonding ability of H atom. Nevertheless, the TSs with two surface atoms being shared by reactants (e.g., TS2 of $\text{N} + \text{H}$ reaction) are still less stable compared to the TSs with only one surface atom being shared (e.g., TS1 of $\text{N} + \text{H}$ reaction).

(ii) The local charge densities of reactants in the reaction direction. As discussed above, the higher the local charge densities in the reactants along the reaction direction would result in a larger Pauli repulsion and consequently leads to a higher barrier. The local charge densities of a re-

actant are determined by the bonding of the reactant with its ligands. Quite often, the valency of reactants is a good measure of the local charge densities (Fig. 4). As we have shown above, for a series of reactions, such as hydrogenation reactions ($\text{C} + \text{H}$, $\text{N} + \text{H}$, $\text{NH} + \text{H}$, $\text{O} + \text{H}$), and oxygenation reactions ($\text{C} + \text{O}$, $\text{N} + \text{O}$, and $\text{O} + \text{O}$) on metals, the lower the valency, the higher the barrier. The local charge densities of reactants are also related to the bonding of the reactants with the surface. When a reactant sits at a lower coordination site, such as a top site, it is more active to react with others owing to the reduction of Pauli repulsion.

(iii) The potential energy surface of the reactant on the surface. In the reactions that the reactants vary the adsorption site from the IS to the TS, the potential energy surface of the reactants may be an important factor to determine the barrier height. The $\text{NH}_2 + \text{H}$ and $\text{OH} + \text{H}$ reactions on metal surfaces are typical examples of this type of reactions.

It should be emphasized that an association reaction on the metal surface usually possesses several different reaction pathways and thus different TSs and barriers, as shown in this work. The three factors discussed above may simultaneously exist in the pathways and the lowest energy pathway should correspond to the best compromise of the three factors. For instance, if one of these factors is very large in a pathway, the pathway is not likely to be the one with the lowest energy: The reaction may “intelligently” avoid this factor and adopt a lower energy pathway, in which all three components may be quite even distributed, as shown in Table IV.

V. CONCLUSIONS

This work represents one of the first systematic studies of hydrogenation reactions on surfaces, an important type of catalytic reactions. We calculated the reactions of $\text{C} + \text{H} \rightarrow \text{CH}$, $\text{N} + \text{H} \rightarrow \text{NH}$, $\text{NH} + \text{H} \rightarrow \text{NH}_2$, $\text{NH}_2 + \text{H} \rightarrow \text{NH}_3$, $\text{O} + \text{H} \rightarrow \text{OH}$ reactions on Rh(111) aiming to address hydrogenation processes in general. In addition, $\text{C} + \text{O} \rightarrow \text{CO}$, $\text{N} + \text{O} \rightarrow \text{NO}$, and $\text{O} + \text{O} \rightarrow \text{O}_2$ on the same surface were also studied to further understand the barrier of surface association reactions. The following results on the reactions were obtained.

(i) The reaction of $\text{C} + \text{H}$, $\text{N} + \text{H}$, $\text{NH} + \text{H}$, and $\text{O} + \text{H}$ reaction achieve similar TSs on Rh(111). There are two TSs for each reaction. At the most stable TS, C, N, NH, O stay at the initial hollow sites to react with H atom. The barriers of the $\text{C} + \text{H}$, $\text{N} + \text{H}$, $\text{NH} + \text{H}$, and $\text{O} + \text{H}$ reactions are 0.72, 1.00, 1.25, and 1.32, respectively, which shows the barrier being a linear function of the valency: The lower the valency of the reactant, the higher the barrier. It was also found that the valency-barrier trend is also present in the series of oxygenation reactions studied, i.e., $\text{C} + \text{O}$, $\text{N} + \text{O}$, and $\text{O} + \text{O}$: The barriers of them are determined to be 1.57, 2.17, and 2.51 eV, respectively.

(ii) The $\text{NH}_2 + \text{H}$ reaction also has two TSs, but the TSs are different from those in the C, N, NH, and O hydrogenation reactions. In the lower energy pathway, NH_2 moves from its initial bridge site to a top site to achieve the TS. The barrier of $\text{NH}_2 + \text{H}$ reaction is calculated to be 1.24 eV, similar to the barrier of $\text{NH} + \text{H}$ reaction.

In this article, we have presented a thorough analysis of association reaction barriers in order to understand the physical origin of the barriers of the hydrogenation reactions. Two major findings are as follows:

(i) For the C, N, NH, and O hydrogenation reactions, the interaction energy between two reactants in the TS plays an important role in determining the trend in the barriers. There are two major components in the interaction energy: the *bonding competition and the direct Pauli repulsion*. The Pauli repulsion effect is responsible for the linear valency-barrier trend in the C, N, NH, and O hydrogenation reactions.

(ii) For the $\text{NH}_2 + \text{H}$ reaction, the energy cost of the NH_2 activation from the IS to the TS is the main part of the barrier. The *potential energy surface* of the NH_2 on metal surfaces is thus crucial to the barrier of $\text{NH}_2 + \text{H}$ reaction.

We have shown that three factors are crucial to the barrier of surface association reactions. The lowest energy pathway should correspond to the best compromise of these three factors. Namely, in the lowest energy pathway the three factors may be quantitatively similar.

ACKNOWLEDGMENTS

We gratefully acknowledge the UKCP for computing time in T3E and the supercomputing center in Ireland for computing time in IBM-SP.

¹G. R. Darling and S. Holloway, Rep. Prog. Phys. **58**, 1595 (1995).

²J. Harris and S. Andersson, Phys. Rev. Lett. **55**, 1583 (1985).

³B. Hammer and J. K. Norskov, Surf. Sci. **343**, 211 (1995).

⁴B. Hammer and J. K. Norskov, Adv. Catal. **45**, 71 (2000).

⁵S. Dahl, A. Logadottir, R. C. Egeberg, J. H. Larsen, I. Chorkendorff, E. Tornqvist, and J. K. Norskov, Phys. Rev. Lett. **83**, 1814 (1999); S. Dahl, P. A. Taylor, E. Tornqvist, and I. Chorkendorff, J. Catal. **178**, 679 (1998).

⁶Z.-P. Liu and P. Hu, J. Chem. Phys. **114**, 8244 (2001); A. Logadottir, T. H. Rod, J. K. Norskov, B. Hammer, S. Dahl, and C. J. H. Jacobsen, J. Catal. **197**, 229 (2001).

⁷Z.-P. Liu and P. Hu, J. Am. Chem. Soc. **125**, 1958 (2003).

⁸G. Henkelman and H. Jonsson, Phys. Rev. Lett. **86**, 664 (2001).

⁹R. I. Masel, *Principles of Adsorption and Reaction on Solid Surface* (Interscience, New York, 1996).

¹⁰K. I. Aika and K. Tamaru, in *Ammonia: Catalysis and Manufacture*, edited by A. Nielsen (Springer-Verlag, Berlin 1995).

¹¹G. Ertl, Catal. Rev.-Sci. Eng. **21**(2), 201 (1980).

¹²S. R. Tennison, in *Catalytic Ammonia Synthesis Fundamentals and Practice*, edited by J. R. Jennings (Plenum, New York, 1991).

¹³G. A. Somorjai, *Introduction to Surface Chemistry and Catalysis* (Wiley, New York, 1994).

¹⁴H. Schulz, Appl. Catal., A **186**, 3 (1999).

¹⁵H. Schulz and M. Claeys, Appl. Catal., A **186**, 91 (1999).

¹⁶Z.-P. Liu and P. Hu, J. Am. Chem. Soc. **124**, 11568 (2002).

¹⁷C. J. Zhang, Z.-P. Liu, and P. Hu, J. Chem. Phys. **114**, 8244 (2001).

¹⁸F. Rosowski, A. Hornung, O. Hinrichsen, D. Herein, M. Muhler, and G. Ertl, Appl. Catal., A **151**, 443 (1997).

¹⁹J. J. Mortensen, Y. Morikawa, B. Hammer, and J. K. Norskov, J. Catal. **169**, 85 (1997).

²⁰K. C. Taylor, Catal. Rev. **35**, 457 (1993).

²¹M. Shelef and G. W. Graham, Catal. Rev. **36**, 433 (1994).

²²W. C. Hecker and A. T. Bell, J. Catal. **84**, 200 (1983).

²³J. P. Perdew, J. A. Chevary, S. H. Vosko, K. A. Jackson, M. R. Pederson, D. J. Singh, and C. Fiolhais, Phys. Rev. B **46**, 6671 (1992); D. Vanderbilt, *ibid.* **41**, 7892 (1990).

²⁴M. C. Payne, M. P. Teter, D. C. Allan, T. A. Arias, and J. D. Joannopoulos, Rev. Mod. Phys. **64**, 1045 (1992).

²⁵For instance, for the $\text{N} + \text{H} \rightarrow \text{NH}$ reaction on Rh(111), a four-layer slab calculation with the top layer being relaxed yields a barrier of 0.97 eV, similar to the 0.99 eV barrier from the three-layer calculation without relaxation.

²⁶Z.-P. Liu and P. Hu, J. Am. Chem. Soc. **123**, 12596 (2001); Z.-P. Liu and P. Hu, J. Chem. Phys. **115**, 4977 (2001).

²⁷Z.-P. Liu and P. Hu, J. Am. Chem. Soc. **124**, 5175 (2002).

²⁸C. J. Zhang and P. Hu, J. Am. Chem. Soc. **122**, 2134 (2000).

²⁹C. J. Zhang and P. Hu, J. Am. Chem. Soc. **121**, 7931 (1999).

³⁰A. Michaelides and P. Hu, J. Am. Chem. Soc. **123**, 4235 (2001).

³¹A. Michaelides and P. Hu, J. Chem. Phys. **114**, 5792 (2001).

³²A. Michaelides and P. Hu, J. Chem. Phys. **115**, 8570 (2001).

³³A. Alavi, P. Hu, T. Deutsch, P. L. Silverstrelli, and J. Hutter, Phys. Rev. Lett. **80**, 3650 (1998).

³⁴K. Bleakley and P. Hu, J. Am. Chem. Soc. **121**, 7644 (1999); M. Lynch and P. Hu, Surf. Sci. **458**, 1 (2000).

³⁵J. J. Mortensen, B. Hammer, and J. K. Norskov, Surf. Sci. **414**, 315 (1998).

³⁶B. Hammer, Phys. Rev. Lett. **83**, 3681 (1999).

³⁷F. Frechard, R. A. van Santen, A. Siokou, J. W. Niemantsverdriet, and J. Hafner, J. Chem. Phys. **111**, 8124 (1999).

³⁸A. Michaelides and P. Hu, J. Am. Chem. Soc. **122**, 9866 (2000).

³⁹P. J. Feibelman, Phys. Rev. B **38**, 12133 (1988).

⁴⁰E. J. Baerends, in *Cluster Models for Surface and Bulk Phenomena*, edited by G. Pacchioni *et al.* (Plenum, New York, 1992).

⁴¹E. C. Egeberg, S. Ullmann, I. Alstrup, C. B. Mullins, and I. Chorkendorff, Surf. Sci. **497**, 183 (2002).